To be published in "Information Processing in the Somatosensory System,"
Eds: O. Franzen, R. Johansson and L. Terenius. Birkhauser Verlag AB, Basel, 1996

# Tactile neural codes for the shapes and orientations of objects

Robert H. LaMotte, Charles Lu and *Mandayam A. Srinivasan

*Department of Anesthesiology, Yale University School of Medicine, 333 Cedar St., New Haven CT 06510 and *Research Laboratory of Electronics, Massachusetts Institute of Technology, Cambridge, Massachusetts, USA*

*Summary.* A series of small, three dimensional objects of differing shape each mounted on a flat plate were constructed. The objects were a cylinder and sphere, each with a 5 mm radius, and two toroids each with a radius of 5 mm along one axis and differing radii of 1 or 3 mm along the orthogonal axis. Using a servocontrolled translation device with 3 degrees of freedom, each object was stroked back and forth across the skin under a maintained compressional force along a series of laterally shifted parallel linear trajectories oriented 90° with respect to the long axis of the finger. The toroid was oriented at 0,30,60 or 90°. Three dimensional "spatial event plots" (SEPs) -discharge rate vs location of object on the receptive field- were obtained for slowly- and rapidly-adapting mechanoreceptive type I fibers (SAs and RAs) with receptive fields centrally located on the fingerpad.

Interpreting the SEPs as responses of a spatially distributed population of fibers, the data supported the following conclusions and hypotheses: (1) The contour of the base of the SEPs of RAs and SAs representing the outline of the region of mechanoreceptor activity in the skin encoded the size, shape and orientation of the two dimensional outline of the object in contact with the skin; (2) The third dimension of shape was represented best in the shape of the distribution of spatial discharge rates (impulses/sec/mm) primarily in the SA fiber population. The shapes of the spatial discharge rates of RAs were more irregular and variable than those of SAs and exhibited poor or no representation of object shape. It was hypothesized that the distribution of slopes of the spatial discharge rate profile evoked by an object in the SA population encoded the distribution of curvatures on the surface of the object in contact with the skin. The constant curvature along the minor axis of a toroidally shaped object was found to be represented by a constant slope along the rising and/or the falling phase of a corresponding cross-section through the spatial discharge rate profile.

## Introduction

The momentary "view" of the shape of an object as it sweeps across the fingerpad is more often described by the perceiver in terms of the object's features rather than its mode of contact with the skin. The spatial distribution of curvatures that define a shape (Gauss, 1827; Srinivasan and LaMotte, 1991) seem to the perceiver to remain constant in the presence of considerable variations in the object's orientation on the skin or its contact force and trajectory. The sensory information required for this perceptual constancy must be contained in the responses of a population of mechanoreceptive

peripheral nerve fibers. So must the information representing the mode of tactile contact. In the following, we describe candidate neural mechanisms by which an object's shape and its orientation on the skin can be separately represented in the responses of these mechanoreceptive primary afferent fibers. The tactile stimuli are toroidal objects that are constructed to differ in radius along one axis and which are stroked across the passive fingerpad at differing orientations with respect to the stroke trajectory.

## Methods

Stimulus objects and method of stimulation. The toroids had a radius of 5 mm along one axis and, for the orthogonal axis, a radius of 1 mm for one toroid and 3 mm for the other. A sphere and a cylindrical bar each had a radius of 5 mm. Thus, for all these specimens, curvature was the same along one axis but different for the other. The first step in producing the toroids and sphere was to use a radius cutting tool to cut a toroid from a rotating cylinder. Then, with the axis of the toroid horizontal, the top of the toroid was cut off along a section parallel to the axis, 0.5mm from the peak. The resulting bump, which had the shape of the top of an egg, was mounted on a flat plate resulting in a toroid "in relief". The outline of the base of this bump was an ellipse. A longitudinal section through the cylinder, 0.5 mm from the surface was mounted to a plate in similar fashion. A given plate containing one of these shapes was mounted on a three-axis load cell attached to a torque motor. The motor was mounted on a three-axis translation table that was used to control the motion of the stimulus object along a linear trajectory in the horizontal plane while the torque motor controlled the compressional force of the object against the skin.

Neural responses to each object stroked across the fingerpad of the anesthetized monkey (macaca fascicularis) were recorded from rapidly adapting type I and slowly adapting type I mechanoreceptive fibers (RAs and SAs respectively) in the median or ulnar nerve. All receptive fields were centrally located on the distal pad of the 2nd, 3rd or 4th fingers. The orientation of the cylindrical bar was held constant at 90° (parallel to the long axis of the finger) whereas the orientations of the two toroids were 90, 60, 30 or 0°. The object was stroked along a direction perpendicular to the axis of the finger

from one side of the receptive field to the other and back along a series of linear parallel trajectories separated by 0.1 or 0.2 mm. The object was first placed proximal to the most sensitive spot in the receptive field and stroked back and forth and then shifted along the orthogonal axis, repeatedly, until reaching the most distal aspect of the receptive field. The overall compressional force was maintained at 10 gwt.

## Results

### Orientation

The responses of a typical SA and RA to each orientation of the thinnest toroid (1 x 5 mm radius) indicate that orientation is encoded in the two-dimensional orientation of the spatial response profiles of both fiber populations (Fig 1A and 1C). Each dot in each spatial event plot (SEP) is the location of the center of the toroid as the object, with indicated orientation, was stroked at 10 mm/s in a single direction in a series of parallel strokes oriented at 0°. We interpret each SEP as the spatially distributed activity of a population of fibers with identical functional properties viewed at the instant in time when the object was centrally located on the finger pad (LaMotte et al., 1994).

The cluster of activity in the center of each SEP changed its orientation in relation to the orientation of the toroid. To measure the orientation of this two-dimensional cluster, we first eliminated the background discharge evoked by the flat plate surrounding the toroid. Principal components analysis (Morrison, 1967) was then used to obtain the orientation of the principal component through the remaining central cluster of data points (Fig. 1B and 1D). In this analysis, the squared distance between each point and the principal component along the orthogonal line is minimized.

The orientation of the toroid was encoded equally well in the responses of RAs and SAs. These neural representations of orientation were closely related to physical orientation. The SEPs of some RAs, while retaining a poor representation of shape, nevertheless exhibited an accurate orientation due to their "off" response to the unloading of the skin as the object moved off the receptive field. The variability in principal components for each fiber type was lowest at 90 and greatest at 0°.

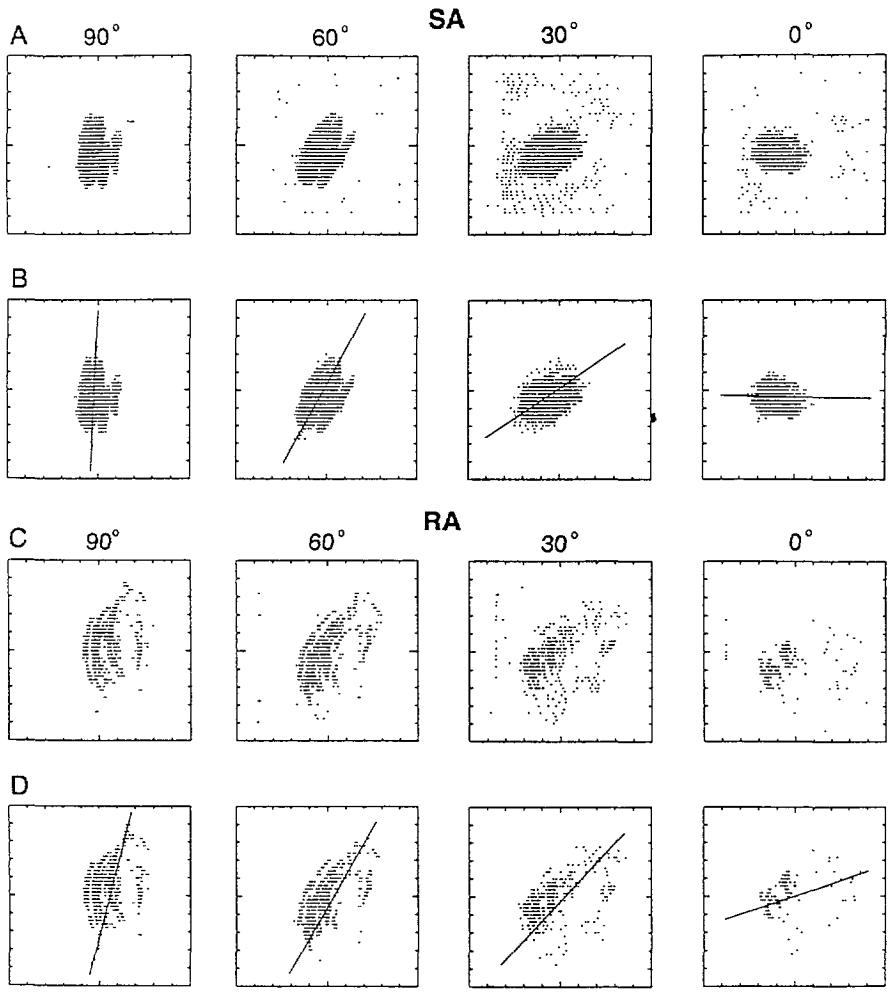


Figure 1. Peripheral neural representation of the orientation of an object stroked across the fingerpad. Spatial event plots of the responses of an SA and RA to different orientations of the thinnest toroid stroked in the same direction across their receptive fields on the fingerpad. The toroid (1 x 5 mm radii) was oriented 90, 60, 30 and 0° to the direction of stroking which was perpendicular to the long axis of the finger. Each dot is the location of the center of the toroid when an action potential occurred. After each stroke from left to right the object was shifted by 0.1 mm proximal to distal (upward in the figure). The contact force was 10 g-wt. and the stroke velocity 10 mm/s. Tic mark spacing on each axis is 1 mm. A and C: Raw data obtained for an SA and RA. B and C: The same data after the background discharges evoked by the pressure of the flat plate and/or skin stretch was eliminated. The solid line in each panel is the major vector, determined by a principle components analysis, that best describes the spatial orientation of the cluster of action potentials evoked by the toroid.

## Shape

The discharge rate of each fiber increased as a function of the curvature of the minor and major axes of the stimulus objects stroked in the same manner over the skin. The cylinder, with zero curvature on its major axis, evoked the lowest rate, followed in order of increasing rate by the sphere and the toroids with 3 x 5 and 1 x 5 mm radii respectively. However, discharge rate did not provide a reliable code for the shape of an object since it could change readily with alterations in contact force, the orientation of the object and the direction and velocity of stroking.

Accordingly, it seemed likely that the shape of an object is encoded in the shape of the spatial response profile of a population of fibers (e.g. LaMotte and Srinivasan, 1987a; Goodwin et al., 1995). One representation of this profile is the two-dimensional SEPs, shown for an SA (Fig. 2A) and an RA (Fig. 2C). These were obtained in response to the two toroids, the sphere and the cylinder each stroked in the same direction along the 0° trajectory. The toroids were oriented at 90°, the contact force was 10 g-wt and the stroke velocity 10 mm/s. The outline of the base of each object mounted on the flat plate is superimposed on the impulse raster. The shape of this outline is the shape of a horizontal cross-section through the object 0.5 mm from the top.

The shape and size of the two dimensional outline of the object in contact with the skin are well represented by the borders of the fiber activity. This was true for RAs as well as SAs. The shape of the object was better defined by the leading side of a fiber's response (left borders for these SEPs) than by the trailing side. The overall curvature of the left border of the dot raster encoded the elliptical shape at the base of the object in contact with the skin. For the objects oriented at 90° it is greatest for the sphere (but was still greater for the toroids oriented at 0°) and least for the cylinder whose border has no curvature as shown in the figure. The vertical length of the region of fiber activity in each SEP and its width at the midportion encode the length and width of the contact area along the major and minor axes of the object. For the stimuli used in these experiments, the contact area, in turn, is directly related to the curvature of the object along these axes. Thus, the width is greatest for the sphere and cylinder with 5 mm radii for minor axes and least for the 1 x 5 mm toroid. The vertical length is greatest for the cylinder (limited to 8 mm by the number of trajectories) and

roughly the same size for the toroid and the sphere each of which had a radius of 5 mm for the major axis.

The third dimension of the shape of each object is likely to be represented by the pressure distribution along the surface of the skin at a given instance in time (Srinivasan and LaMotte, 1991). To study the shape of the spatial response profile generated by this distribution, the spatial discharge rate, defined as the number of impulses/0.2 mm bin) was plotted on a vertical axis perpendicular to the SEP in the horizontal plane. An average of the middle five cross-sections (parallel to the direction of stroking) through this three-dimensional SEP is shown for the same SA in Fig. 2B. The peak spatial discharge rate was lowest for the cylinder and increased with increasing curvature of the minor axis from the sphere to the thinner toroid. When the same curves were normalized with respect to their respective peak discharge rates, the four spatial response profiles were still discriminable on the basis of their base widths and the rates of decline from peak to base on the trailing side of the profile (and for some SAs, the rates of ascent from base to peak on the leading side). As the curvature along the minor axis of an object increased, the base widths decreased. For most fibers, these response profiles were more or less triangular and a straight line appeared, as a first approximation, to be the most reasonable fit to the ascending or the declining phase of each profile. Accordingly, as a gross estimate of the rate of ascent and decline of each profile, a straight line was fitted to the data from base to peak, and another line from peak to base. The slopes of the lines for the declining phases were found to increase with the curvature of the minor axis for the four objects for the majority of the SAs tested. A similar relationship between slope and curvature was obtained in a minority of SAs for the rising phase as well. Similar results, however, were not obtained for either phase for RAs whose spatial response profiles were much more irregular and variable in comparison with those of SAs (Fig. 2D). The shape of the RA response profiles deteriorated further when the stroke velocity was lowered to 5 mm/s (not shown) which, for some RAs, evoked only a few impulses per stroke. In contrast, the shapes of the spatial response profiles of SAs were more robust in encoding object shape in the presence of changes in stroke velocity.

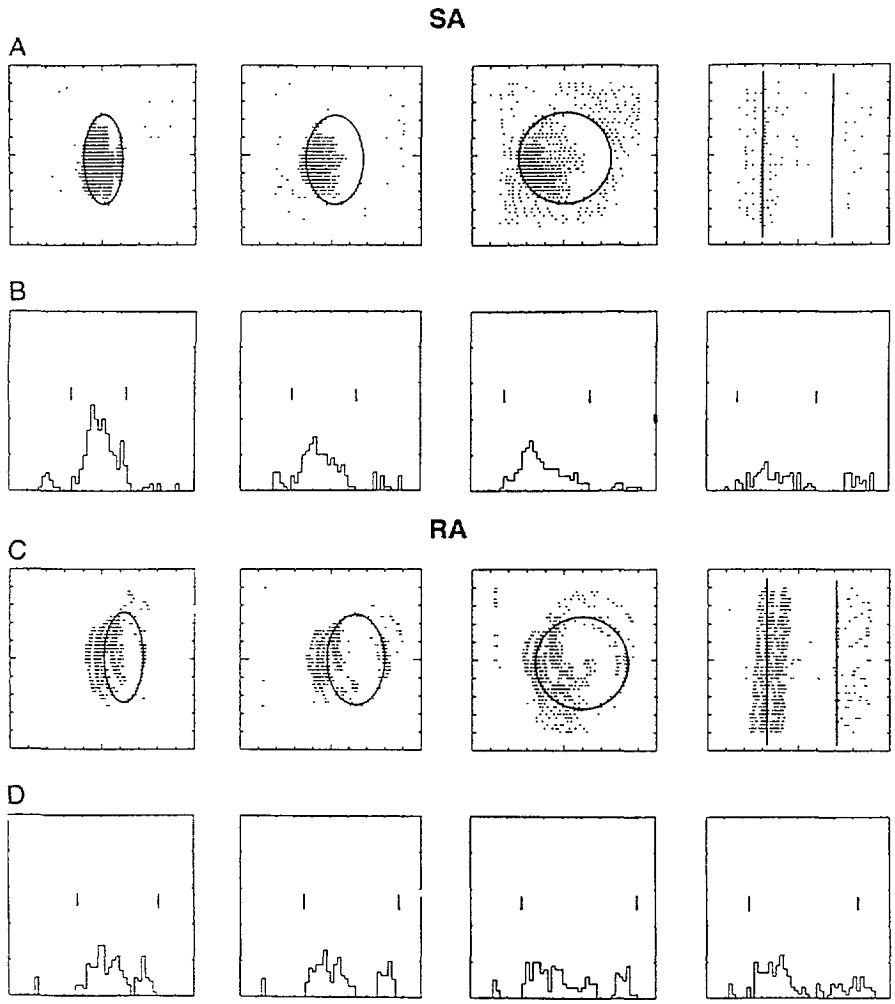


Figure 2. Peripheral neural representations of the shapes of objects stroked across the fingerpad. Spatial event plots of the responses of an SA and RA to objects of the same orientation but different shape stroked in the same direction across their receptive fields on the fingerpad. A and C: Same format as A and C in Fig. 1. The shape of the base of each object on the flat plate is superimposed. This is the outline of a horizontal cross-section through the shape 0.5 mm from the top. B and D: The spatial discharge rate (impulses/0.2 mm bin) on the vertical axis was averaged from the data obtained from five consecutive strokes located in the middle of the shape or cluster of action potentials evoked by the object (data in each panel obtained from panel directly above). The two vertical tic marks directly above each histogram delineate the beginning and end of the cluster of impulses evoked by the object itself as opposed to background discharge produced by the plate.

## Discussion

Human subjects can readily discriminate differences in the curvature of small shapes pressed against (Srinivasan and LaMotte, 1987; Goodwin et al., 1991) and stroked across (LaMotte and Srinivasan, 1987a) the fingerpad on the basis of tactile cues alone. Similarly, proprioceptive information is not required to tactually identify, with little or no error, up to six categories of orientation of a thin (1 x 5 mm radii) toroid pressed against the stationary fingerpad (LaMotte et al., 1992).

The results obtained in the present experiments provide a basis for hypothesizing how the three-dimensional shape and orientation of an object stroked across the fingerpad are separately encoded in the evoked responses of SA and RA mechanoreceptive cutaneous afferent fibers. The features of shape and object orientation cannot be encoded solely in the pattern or rate of discharges in individual afferent fibers. These rates could be altered to the same degree by appropriate variations in curvature or orientation as they could by changes in shape. In addition, discharge rates are also greatly influenced by changes in the contact force of an object (Goodwin et al., 1995) as well its velocity and direction of stroking (LaMotte and Srinivasan, 1987a,b). Instead, the properties of shape and orientation must be coded in the responses of populations of mechanoreceptive afferent fibers.

The central portion of each two-dimensional SEP was interpreted as representing the spatial distribution of activity evoked by the object in a population of SAs and RAs at an instance in time. The area, two dimensional shape and orientation of this region of afferent activity encode, respectively, the size, shape and orientation of that region of the object in contact with and parallel to the surface of the skin. The parameters of size, two dimensional contact region and orientation of an object appeared to be represented equally well in the spatial response profiles of SA and RA populations. The curvature of the leading edge of the spatial response profiles increased and the width of the response decreased with increasing curvature of the object in the horizontal plane parallel to the skin. The neural representation of object orientation was better when the major axis was perpendicular rather than parallel to the direction of stroking. This is likely to be due to the greater magnitude and rate of change in the curvature of the skin produced by the object, and greater fiber discharge rates, for strokes along the axis of greater object curvature.

The third dimension of shape, responsible for a characteristic spatial distribution of pressures on the skin, was represented best in the shape of the distribution of spatial discharge rates (impulses/sec/mm) primarily in the SA fiber population. The shapes of the spatial distribution of discharge rates of RAs were more irregular and variable than those of SAs and exhibited poor or no representations of object shape. It is hypothesized that the distribution of slopes of the spatial discharge rate profile evoked by an object in the SA population encodes the distribution of curvatures on the surface of the object in contact with the skin. The curvature along the minor or major axis of toroidally shaped objects (including cylinders and spheres) is a constant. A constant curvature, then, is represented by a constant slope along the rising and/or falling phase of a corresponding cross-section through the spatial discharge rate profile. In the present experiments this profile was tent-shaped and was generated primarily by the leading edge of the object stroked across the skin. Thus, the representation of three-dimensional shape in the responses of primary afferent fibers is not isomorphically related to the physical shape of the object stroked across the skin. A greater degree of isomorphism in neural representation is obtained when pressing but not stroking a three-dimensional object (Goodwin et al., 1995) against the skin or when stroking a two-dimensional forms represented by a pattern of elements in a horizontal plane (Johnson and Lamb, 1981).

The progression of increasing curvatures from the sphere to the thinner of the two toroids produced correspondingly steeper, constant slopes on the falling phases of the spatial response profiles. Differences in object curvature were represented more consistently by changes in the slope of the declining portion of this profile more often than in the rising part. This is possibly due to a greater response variability from transient mechanical events generated by the sudden impact of the toroidal shapes (especially those with small radii) on a plate that has already reached the desired velocity by the time the object in relief reaches the most sensitive spot in a fiber's receptive field. More symmetrical "tent-shaped" profiles of spatial discharge rate were obtained from SAs in response to an aperiodic wavy surface stroked across the skin (unpublished observations and LaMotte et al., 1994). The wavy surface consisted of a sequence of alternating convex and concave cylinders (with radii of 3.1 to 16.9 mm) and constructed to have a continuously changing surface slope. These

curvatures were generally larger and more smoothly changing than those used in the present experiments. Similarly, symmetrical tent shaped spatial discharge rate profiles were obtained from SAs in response to spheres of differing curvature pressed against the fingerpad (Goodwin et al., 1995).

## References


Gauss, C.F. (1827) Disquisitiones generales circa superficies curvas. *Commentationes Societatis Regiae ScientiarumGottingenesis Recentiores.* 6:99-146.

Goodwin, A.W., Browning, A.S. and Wheat, H.E. (1995) Representation of curved surfaces in responses of mechanoreceptive afferent fibers innervating the monkey's fingerpad. *J. Neurosci.* 15:798-810.

Goodwin, A.W., K.T. John, and A.H. Marceglia (1991) Tactile discrimination of curvature by humans using only cutaneous information from the fingerpads. *Exp. Brain Res.* 86:663-672.

Goodwin,A.W., and H.E. Wheat (1992) Magnitude estimation of contact force when objects with different shapes are applied passively to the fingerpad. *Somatosen. and Motor Res.*:9, 339-344.

Johnson, K.O. and Lamb, G.D. (1981) Neural mechanisms of spatial tactile discrimination: neural patterns evoked by Braille-like dot patterns in the monkey. Journal of Physiology (London) 310, 117-144

LaMotte, R.H., and M.A. Srinivasan (1987a) Tactile discrimination of shape: Responses of slowly adapting mechanoreceptive afferents to a step stroked across the monkey fingerpad. *J. Neurosci.* 7:1655-1671.

LaMotte, R.H., and M.A. Srinivasan (1987b) Tactile discrimination of shape: Responses of rapidly adapting mechanoreceptive afferents to a step stroked across the monkey fingerpad. *J. Neurosci.* 7:1672-1681.

LaMotte, R.H., M.A. Srinivasan and A. Klusch-Petersen. (1992) Tactile discriminations and identifications of different shapes and orientations of ellipsoidal objects applied to the fingerpad. *Soc. Neurosci. Abstr.* 18:830.

LaMotte, R.H., M.A. Srinivasan, C. Lu, and A. Klusch-Petersen (1994) Cutaneous neural codes for shape. *Can. J. Physiol. Pharm.* 72:498-505.

Morrison, D.F. (1967) The Structure of Multivariate Observations: I. Principal Components. In: *Multivariate Statistical Methods.* McGraw-Hill, New York. pp. 221-258.

Srinivasan, M.A., and R.H. LaMotte (1987) Tactile discrimination of shape: Responses of slowly and rapidly adapting mechanoreceptive afferents to a step indented into the monkey fingerpad. *J. Neurosci.* 7:1682-1697.

Srinivasan, M.A., and R.H. LaMotte (1991) Encoding of shape in the responses of cutaneous mechanoreceptors. *In:* O. Franzen, and J. Westman (eds.): *Information Processing in the Somatosensory System*, MacMillan, London, pp.59-69.